The Plant Cell, Vol. 20: 353–366, February 2008, www.plantcell.org © 2008 American Society of Plant Biologists

An Inositol Polyphosphate 5-Phosphatase Functions in PHOTOTROPIN1 Signaling in *Arabidopis* by Altering Cytosolic Ca^{2+} [W]

Xu Chen,[a,1] Wen-Hui Lin,[a,b,1] Yuan Wang,[a] Sheng Luan,[a,b] and Hong-Wei Xue[a,2]

[a] Shanghai Institutes for Biological Science–University of California Berkeley Center of Molecular Life Sciences, National Key Laboratory of Plant Molecular Genetics, Institute of Plant Physiology and Ecology, Chinese Academy of Sciences, 20032 Shanghai, China

[b] Department of Plant and Microbial Biology, University of California, Berkeley, California 94720

Inositol polyphosphate 5-phosphatase (5PTase) is a key enzyme in the phosphatidylinositol metabolic pathway, which plays critical roles in a number of cellular processes in plants. Our previous work implicated the role of *5PTase13*, which encodes a WD40-containing type II 5PTase, in hormone-mediated cotyledon vein development. Here, we show that *5PTase13* is also involved in blue light responses in *Arabidopsis thaliana*. Compared with that in darkness, the expression of *5PTase13* was suppressed by blue light irradiation, and disruption of the gene resulted in shortened hypocotyls and expanded cotyledons. Genetic analysis showed that *5PTase13* acted independently from *CRYPTOCHROME1* and *CONSTITUTIVE PHOTOMORPHOGENIC1* but interacted functionally with *PHOTOTROPIN1* (*PHOT1*). The expression level of *5PTase13* was significantly enhanced in *phot1* single or *phot1 phot2* double mutants under blue light, and suppression of *5PTase13* expression rescued the elongated hypocotyls in the *phot1* or *phot1 phot2* mutants. Further analysis showed that the blue light–induced elevation of cytosolic Ca^{2+} was inhibited in the *phot1* mutant but enhanced in the *5pt13* mutant, suggesting that *5PTase13* antagonizes *PHOT1*-mediated effects on calcium signaling under blue light.

INTRODUCTION

Plants have evolved a number of mechanisms for responding to a broad spectrum of light through activation of specific sets of photoreceptors (Franklin et al., 2005; Wang, 2005). Recent studies have characterized the phytochrome family of red/far-red light receptors (Schepens et al., 2004; Kim et al., 2005; Rockwell et al., 2006), the cryptochrome (CRY) family of blue light receptors (Lin and Todo, 2005; Li and Yang, 2007), and the phototropin (PHOT) family of blue light receptors (Kimura and Kagawa, 2006).

Arabidopsis thaliana mutants *cry1* and *cry2* exhibit elongated hypocotyls, and the *CRY1* and *CRY2* gene products have been identified as blue light receptors that mediate light-dependent inhibition of hypocotyl elongation. Studies have also shown that CRY1 is negatively regulated by CONSTITUTIVE PHOTOMORPHOGENIC1 (COP1; a photomorphoregenesis repressor) (Ang et al., 1998) through the interaction of the C-terminal region of CRY1 and the WD40 repeats of COP1 (Yang et al., 2001). In addition, PHOT1 and PHOT2, both of which are Ser/Thr photoreceptor kinases that undergo autophosphorylation in response to blue light (Cho et al., 2007; Christie, 2007), represent another class of blue light receptor controlling plant phototropism, chloroplast orientation, stomatal opening, and rapid inhibition of growth of *Arabidopsis* etiolated seedlings (Briggs and Christie, 2002; Briggs, 2007; Cho et al., 2007).

The phototropin proteins carry two domains: a C terminus–localized Ser/Thr kinase domain and an N terminus–localized LOV domain (Kasahara et al., 2002; Franklin et al., 2005). Four phototropin-interacting proteins have been identified in *Arabidopsis*, namely, NON-PHOTOTROPIC HYPOCOTYL3 (Motchoulski and Liscum, 1999; Pedmale and Liscum, 2007), ROOT PHOTOTROPISM2 (RPT2; Inada et al., 2004), PHYTOCHROME KINASE SUBSTRATE1 (Lariguet et al., 2006), and a 14-3-3 protein (Kinoshita et al., 2003), and a fifth in *Vicia faba*, phot1A-interacting protein (Emi et al., 2005). These five proteins participate in the regulation of phototropic responses (Liscum and Briggs, 1995, 1996; Motchoulski and Liscum, 1999; Sakai et al., 2000; Inada et al., 2004), chloroplast movement (Inada et al., 2004), and stomatal aperture control (Lascève et al., 1999; Inada et al., 2004). Other studies have shown that calcium might be part of the blue light signaling pathway (Baum et al., 1999; Babourina et al., 2002; Folta et al., 2003; Stoelzle et al., 2003; Christie, 2007; Harada and Shimazaki, 2007).

Calcium, a universal second messenger, is involved in diverse cellular functions and is crucial in cell responses to a variety of stimuli (Luan et al., 2002; Yang and Poovaiah, 2003), including circadian oscillations (Xu et al., 2007), gravity (Poovaiah et al., 2002), stresses (Quan et al., 2007), and hormones (Du and Poovaiah, 2005). In particular, studies have revealed the importance of cytosolic Ca^{2+} concentration ($[Ca^{2+}]_{cyt}$) in photomorphogenesis (Harada and Shimazaki, 2007). Blue light induces opening of anion and potassium channels (Cho and Spalding, 1996; Suh et al., 2000), resulting in the change of $[Ca^{2+}]_{cyt}$ (Baum et al., 1999). When plants respond to initial blue light illumination,

[1] These authors contributed equally to this work.

[2] Address correspondence to hwxue@sibs.ac.cn.

The author responsible for distribution of materials integral to the findings presented in this article in accordance with the policy described in the Instructions for Authors (www.plantcell.org) is: Hong-Wei Xue (hwxue@sibs.ac.cn).

[W] Online version contains Web-only data.

www.plantcell.org/cgi/doi/10.1105/tpc.107.052670

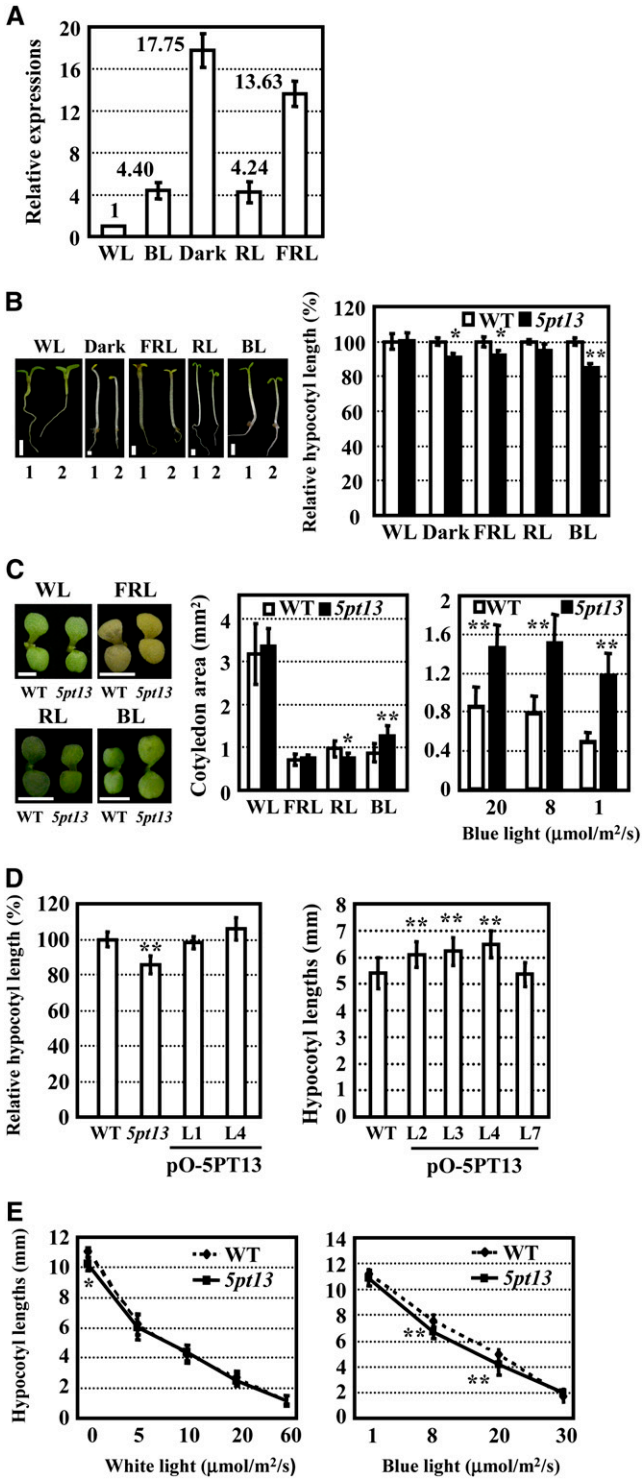

Figure 1. Expression of 5PTase13 Is Regulated by Light, and 5pt13 Mutants Are Less Sensitive to Blue Light.

(A) Expression of *5PTase13* under different light spectra. *5PTase13* mRNA levels were measured under dark, far-red light (FRL; 30 μmol/m²/s), blue light (BL; 20 μmol/m²/s), red light (RL; 30 μmol/m²/s), and white light (WL; 60 μmol/m²/s), respectively.

a transient $[Ca^{2+}]_{cyt}$ elevation is detected that is dependent on PHOT1 (Folta et al., 2003) or both PHOT1 (at lower fluence rates) and PHOT2 (at higher fluence rates) (Harada et al., 2003). Blue light–induced calcium influx is also critical for the primary inhibition of hypocotyl growth but not for phototropism (Folta et al., 2003). However, 30 min after blue light illumination, further inhibition of hypocotyl elongation mostly depends on the CRY1-COP1–mediated ubiquitination pathway (Parks et al., 1998; Folta and Spalding, 2001). Participation of several calcium-regulated factors in the regulation of hypocotyl elongation under red or blue light has been validated. For example, SHORT UNDER BLUE LIGHT1, a Ca^{2+} binding protein, acts as a negative regulator of blue light signaling downstream of CRY1 and CRY2 (Guo et al., 2001). The Ser/Thr protein phosphatase PP7, which binds calmodulin in a Ca^{2+}-dependent manner, functions as a positive regulator of cryptochrome signaling in *Arabidopsis* (Møller et al., 2003). Despite accumulating evidence of calcium involvement in light signaling, there is a missing link between the photoreceptors and the calcium second messenger.

Phosphatidylinositols play crucial roles in multiple developmental processes, including hormone effects (Lin et al., 2004, 2005; Tan et al., 2007; Xue et al., 2007), cytoskeleton architecture (Sechi and Wehland, 2000), ion transport (Liu et al., 2005), stress responses (Williams et al., 2005), and light regulation (Qin et al., 2005). Inositol polyphosphate 5-phosphatases (5PTases) hydrolyze the phosphate group at the 5′ position of the inositol ring and are key enzymes involved in phosphatidylinositol signaling. The distinct substrates of 5PTases are water-soluble inositol polyphosphates, including inositol 1,4,5-trisphosphate [Ins(1,4,5)P_3], inositol 1,3,4,5-tetraphosphate [Ins(1,3,4,5)P_4], and membrane-bound phosphoinositides, such as phosphatidylinositol 4,5-bisphosphate [PtdIns(4,5)P_2] and phosphatidylinositol 3,4,5-trisphosphate. There are 15 genes encoding 5PTases in

(B) Hypocotyl length (left panels; bars = 1 mm) and statistical analysis (right panel) of wild-type and *5pt13* mutant seedlings under dark, far-red light (30 μmol/m²/s), or blue light (20 μmol/m²/s). Five-day-old seedlings were measured and statistically analyzed using a Student's *t* test (*, $P < 0.05$; **, $P < 0.01$). Data represent mean ± SE ($n > 30$). Same-age seedlings were used for all hypocotyl measurements throughout this study. The same procedure, data analysis, and presentation were used for production of all panels.

(C) Images of cotyledons (left panels; bars = 1 mm) and statistical analysis (middle panel) indicated the enlarged cotyledons of *5pt13* under red light (30 μmol/m²/s) or blue light (20 μmol/m²/s). The *5pt13* mutant plants showed enlarged cotyledons under different fluence rates of blue light (1, 8, or 20 μmol/m²/s; right panels). Cotyledons of 5-day-old seedlings were measured and statistically analyzed using a Student's *t* test (*, $P < 0.05$; **, $P < 0.01$). Data represent mean ± SE ($n > 20$).

(D) Overexpression of *5PTase13* in *5pt13* (left panel) or wild-type (right panel) plants resulted in an elongated hypocotyl. Hypocotyls of 5-d-old seedlings grown under blue light (20 μmol/m²/s) were measured and statistically analyzed using a one-tailed Student's *t* test (*, $P < 0.05$; **, $P < 0.01$). Data represent mean ± SE ($n > 30$).

(E) The *5pt13* seedlings had shortened hypocotyls under blue light with different fluence rates (1, 8, 20, or 30 μmol/m²/s; right panel) compared with those grown under white light (left panel). Hypocotyl lengths of 5-d-old seedlings were measured and statistically analyzed using a Student's *t* test (**, $P < 0.01$). Data represent mean ± SE ($n > 30$).

Arabidopsis that are grouped into two subfamilies based on protein structure: type I (11 members) and type II (four members) (Zhong et al., 2004).

Through genetics approaches, several 5PTases, especially type I members, have been functionally characterized in *Arabidopsis*, revealing their diverse functions in various aspects of plant growth and development. Disruption of *5PTase1* increased sensitivity to abscisic acid treatment (Berdy et al., 2001; Gunesekera et al., 2007). *5PTase1* and *5PTase2* regulate germination and early seedling development through altering the Ins(1,4,5)P_3 level (Gunesekera et al., 2007). *COTYLEDON VEIN PATTERN2* (*CVP2*/*5PTase6*) is essential for closed venation patterns of foliar organs through modulating the Ins(1,4,5)P_3 level (Carland and Nelson, 2004). *root hair morphogenesis3* (*mrh3*/*5ptase5*) mutants have altered root hair initiation (Jones et al., 2006). Of the type II members, *FRAGILE FIBER3* (*FRA3*/*5PTase12*) is required for secondary wall synthesis and actin organization in fiber cells (Zhong et al., 2004), and our previous research has shown that *5PTase13* is required for cotyledon vein development through regulating auxin homeostasis (Lin et al., 2005). Here, we identify a role for *5PTase13* in blue light responses and demonstrate crosstalk between *PHOT1* and *5PTase13* through the regulation of the calcium transients under blue light.

RESULTS

Blue Light Suppresses 5PTase13 Expression and 5pt13 Mutants Display Shortened Hypocotyls and Expanded Cotyledons in Response to Blue Light Irradiation

Our previous studies have shown that *5PTase13* expression is differentially regulated under light and dark (Lin et al., 2005). To further investigate the effects of different light spectra on *5PTase13* gene expression, we examined *5PTase13* transcripts under different light spectra through quantitative RT-PCR analysis. As shown in Figure 1A, expression of *5PTase13* was higher in dark-grown seedlings compared with those grown under light. Histochemical analysis of transgenic plants harboring the *5PTase13* promoter-β-glucuronidase (GUS) reporter gene confirmed that expression of *5PTase13* in hypocotyls was inhibited by light at the level of transcription (see Supplemental Figure 1 online).

We further analyzed seedling growth of a *5PTase13* knockout mutant, *5pt13*, under various light conditions and observed a small but significant change in blue light–induced hypocotyl shortening in mutant compared with wild-type seedlings. Although the *5pt13* seedlings showed shorter hypocotyls under both dark and light conditions, the hypocotyl shortening phenotype of the mutant was most significant under blue light (Figure 1B). In addition, *5pt13* mutant cotyledons were smaller than the wild type under red light but larger under blue light (Figure 1C, left and middle panels). Under white light or far-red light, there were no significant differences between the mutant and wild type. These results suggest that the *5pt13* mutant may have altered light responses, especially with regard to blue light. Overexpression of *5PTase13* in *5pt13* plants complemented the mutant phenotype under blue light (Figure 1D, left panel; see Supplemental Figure 2A online), indicating that the changes in blue light responses in the mutant were a result of disruption in the *5PTase13* gene. In addition, transgenic wild-type plants that overexpressed *5PTase13* displayed longer hypocotyls under blue light (see Supplemental Figure 2B online; Figure 1D, right panel), further confirming the effects of *5PTase13* on hypocotyl elongation under blue light.

Table 1. Hybridization with *Arabidopsis* ATH1 Chips Revealed That Deficiency of *5PTase13* Altered the Expression of Genes Involved in Light and Calcium Signal Transduction and Cation Transport

Probe Set	Locus No.	Regulation	Descriptions
259866_at	At1g76640	I (3.3)*	Calmodulin-related protein, putative
260881_at	At1g21550	I (3)**	Calcium binding protein, putative
258181_at	At3g21670	I (3)**	Nitrate transporter (NTP3)
266672_at	At2g29650	I (2.1)**	Inorganic phosphate transporter, putative
248910_at	At5g45820	I (2.1)**	CBL-interacting protein kinase 20 (CIPK20)
267516_at	At2g30520	I (2.2)**	Signal transducer of phototropic response (RPT2)
253172_at	At4g35060	I (2.2)*	Heavy metal–associated domain-containing protein/copper chaperone (CCH) related
263779_at	At2g46340	I (1.7)**	Suppressor of phytochrome A-105 (SPA1)
258321_at	At3g22840	I (1.7)**	Chlorophyll A/B binding family protein/early light-induced protein (ELIP)
258239_at	At3g27690	I (1.6)**	Chlorophyll A/B binding protein (LHCB2:4)
262940_at	At1g79520	I (1.6)*	Cation efflux family protein
258350_at	At3g17510	I (1.5)**	CBL-interacting protein kinase 1 (CIPK1)
259970_at	At1g76570	I (1.1)**	Chlorophyll A/B binding family protein
260308_at	At1g70610	I (1)*	ABC transporter (TAP1)

Data were obtained from the aerial organs of wild-type and *5pt13* seedlings as described in Methods. Results are presented as increased (I) expression in *5pt13* seedlings relative to the wild type, and numbers in parentheses indicate the fold change (log_2, with false discovery rate [FDR] values <0.01 [**] or <0.05 [*]).

More detailed analysis of hypocotyl lengths revealed no significant difference between the wild type and the *5pt13* mutant under white light at various fluence rates (5, 10, 20, and 60 μmol/m^2/s; Figure 1E, left panel). The *5pt13* mutant seedlings had significantly shorter hypocotyls under blue light at the fluence rates of 8 or 20 μmol/m^2/s but not at lower or higher fluence rates (Figure 1E, right panel). In addition, enlarged cotyledons were observed under blue light at different fluence rates (1, 8, or 20 μmol/m^2/s; Figure 1C, right panel). Taken together, these results suggest that *5PTase13* participates in blue light–mediated regulation of seedling growth under a specific range of blue light fluence rates.

Consistent with the above observations, analysis of transcription profiling revealed altered expression of many light-regulated genes in *5pt13* mutant seedlings compared with those in wild-type seedlings under white light (chip hybridization was described in Lin et al., 2005). These genes, including those encoding EARLY LIGHT-INDUCED PROTEIN (Casazza et al., 2005), SUPPRESSOR OF PHYTOCHROME A (SPA; Hoecker and Quail, 2001; Laubinger et al., 2004), and CHLOROPHYLL A/B BINDING protein (Meehan et al., 1996), were stimulated under *5PTase13* deficiency (Table 1), suggesting that *5PTase13* functions as a negative regulator of light responses. In addition, expression of cell wall synthesis and cytoskeleton-related genes, especially those encoding UDP-glucosyl transferase family proteins (Reiter, 2002) and xyloglucan:xyloglucosyl transferase (Yokoyama et al., 2004; Cosgrove, 2005), were suppressed in *5pt13* seedlings (Table 2), consistent with the finding that *5PTase13* participates in the regulation of hypocotyl growth.

5PTase13 Acts Independently from CRY1-COP1 but Interacts Functionally with PHOT1

Disruption of *5PTase13* led to changes in blue light responses, including a change in hypocotyl growth. As a blue light receptor, CRY1 plays a key role in the regulation of hypocotyl elongation. Interestingly, COP1, an E3 ligase, regulates blue light response by interacting directly with CRY1. In addition, both COP1 and 5PTase13 contain WD40 repeat domains, which are involved in protein–protein interaction. These observations prompted us to test if there might be functional interactions between 5PTase13 and the other two proteins. We tested for protein–protein interactions using a yeast two-hybrid system and found that 5PTase13 did not interact with either CRY1 or COP1 (Figure 2A). Further genetic analysis of a *5pt13 cry1* double mutant showed that, except for a small proportion (3 to 5%) of seedlings that exhibited long hypocotyls (*cry1* mutants) or shortened hypocotyls (*5pt13* mutants), the majority (>90%) of seedlings had

Table 2. Hybridization with *Arabidopsis* ATH1 Chips Revealed That Deficiency of *5PTase13* Suppressed the Expression of Cell Wall Synthesis and Cytoskeleton-Related Genes

Probe Set	Locus No.	Regulation	Descriptions
259507_at	At1g43910	D (−5.7)**	AAA-type ATPase family protein
266877_at	At2g44570	D (−3.9)*	Glycosyl hydrolase family 9 protein
251791_at	At3g55500	D (−2.3)**	Expansin, putative (EXP16)
260592_at	At1g55850	D (−2.3)**	Cellulose synthase family protein
262643_at	At1g62770	D (−2.1)**	Invertase/pectin methylesterase inhibitor family protein
262978_at	At1g75780	D (−1.9)**	Tubulin β-1 chain (TUB1)
247189_at	At5g65390	D (−1.8)**	Arabinogalactan protein (AGP7)
252625_at	At3g44750	D (−1.7)**	Histone deacetylase, putative (HD2A)
263207_at	At1g10550	D (−1.7)**	Xyloglucan:xyloglucosyl transferase
257206_at	At3g16530	D (−1.7)**	Legume lectin family protein
255433_at	At4g03210	D (−1.7)**	Xyloglucan:xyloglucosyl transferase
258369_at	At3g14310	D (−1.7)*	Pectinesterase family protein
265499_at	At2g15480	D (−1.7)*	UDP-glucoronosyl/UDP-glucosyl transferase family protein
253879_s_at	At4g27570	D (−1.6)**	Glycosyltransferase family protein
261046_at	At1g01390	D (−1.6)**	UDP-glucoronosyl/UDP-glucosyl transferase family protein
263184_at	At1g05560	D (−1.5)**	UDP-glucose transferase (UGT75B2)
245052_at	At2g26440	D (−1.5)*	Pectinesterase family protein
257667_at	At3g20440	D (−1.5)*	Glycoside hydrolase family 13 protein
255070_at	At4g09020	D (−1.4)**	Putative/starch debranching enzyme
265340_at	At2g18330	D (−1.4)**	AAA-type ATPase family protein
257203_at	At3g23730	D (−1.3)**	Xyloglucan:xyloglucosyl transferase
252997_at	At4g38400	D (−1.3)*	Expansin family protein (EXPL2)
261825_at	At1g11545	D (−1.3)*	Xyloglucan:xyloglucosyl transferase
261934_at	At1g22400	D (−1.2)**	UDP-glucoronosyl/UDP-glucosyl transferase family protein
247246_at	At5g64620	D (−1.2)*	Invertase/pectin methylesterase inhibitor family protein
261813_at	At1g08280	D (−1.2)*	Glycosyl transferase family 29 protein
254785_at	At4g12730	D (−1)**	Fasciclin-like arabinogalactan protein (FLA2)

Results are presented as decreased (D) expression in *5pt13* seedlings relative to the wild type, and numbers in parentheses indicate the fold change (log_2, with FDR values <0.01 [**] or <0.05 [*]). The hybridization performance and data analysis are as described in Methods.

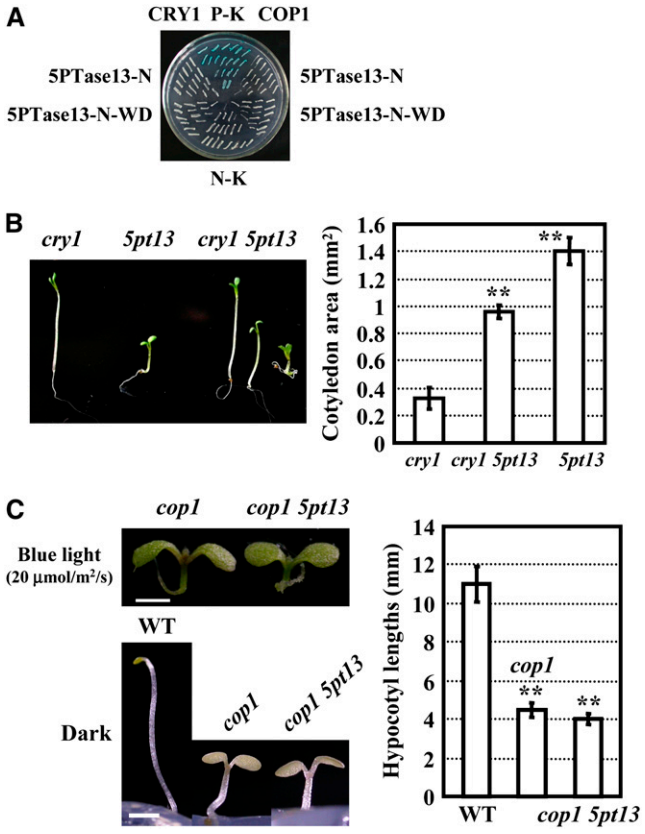

Figure 2. 5PTase13 Functions Independently of COP1 and CRY1.

(A) Yeast two-hybrid analysis showed no interaction between 5PTase13 and COP1 or CRY1. Interaction between the N-terminal region (until the position before WD40 region) or N-WD40 fragment (until the position at end of the WD40 region) of 5PTase13 with COP1 or CRY1 proteins was determined, respectively. The known interaction between pJG4-5-COP1 and pEG202-CCT1 (CRY1 C-terminal) was used as a positive control (P-K). The interaction between empty vectors pEG202 and pJG4-5 was used as the negative control (N-K).

(B) *cry1 5pt13* double mutants had an intermediate phenotype, indicating that there was no direct link between *CRY1* and *5PTase13*. Hypocotyl lengths were measured and data presented as described in Figure 1B.

(C) *cop1 5pt13* double mutants exhibited a *cop1* phenotype, indicating that *COP1* either acts downstream of *5PTase13* or they have no functional relationship. Hypocotyl lengths were measured and data presented as described in Figure 1B.

hypocotyls of an intermediate length (Figure 2B), indicating functional independence of *CRY1* and *5PTase13*. Additionally, the *5pt13 cop1* double mutant had a similar phenotype to *cop1* (Figure 2C), suggesting that *COP1* either acts downstream of *5PTase13* or they have no functional relationship.

In addition to CRY1 and COP1, other photoreceptors, such as PHOT1 and PHOT2, have been identified as functioning in blue light responses (Briggs and Christie, 2002; Briggs, 2007; Cho et al., 2007). PHOT1 is involved in blue light–mediated hypocotyl growth inhibition through stimulating an increase in $[Ca^{2+}]_{cyt}$ (Folta et al., 2003). Because the expression level of *5PTase13* is regulated by blue light, we decided to measure *5PTase13* expression in the *phot1* and *phot2* single mutants and the *phot1 phot2* double mutant to determine if these blue light receptors are involved in the regulation of *5PTase13* expression. As shown in Figure 3A, under blue light, the transcript level of *5PTase13* in the *phot1* or *phot1 phot2* double mutants was much higher than that in the wild-type plants, increasing 25- and 12-fold, respectively, whereas no significant change was detected in the *phot2* mutant (Figure 3A, left). This result indicates that PHOT1 may be the major blue light receptor mediating blue light–induced repression of *5PTase13* gene expression.

Further studies employing genetic epistatic analysis showed that under blue light, *phot1 5pt13* double mutant plants exhibited shortened hypocotyls similar to *5pt13* (Figure 3B), suggesting that *5PTase13* may act downstream of *PHOT1* and serve as a negative regulator in blue light signaling. In addition, *phot1* single mutant or *phot1 phot2* double mutant seedlings with reduced levels of *5PTase13* (due to transgenic expression of antisense RNA) exhibited shortened hypocotyls under blue light (Figures 3C and 3D, right panels), similar to the *phot1 5pt13* double mutant seedlings. By contrast, overexpressing *5PTase13* in *phot1* seedlings enhanced the long hypocotyl phenotype of the *phot1* mutant under blue light (Figure 4A), further supporting the hypothesis that *5PTase13* functions downstream of *PHOT1* as a negative regulator of the blue light response. Similar transgenic analysis with *phot2* showed no affect on the hypocotyl length of *phot2* (Figure 4B), indicating there may not be a functional link between *PHOT2* and *5PTase13*. Additionally, the yeast two-hybrid assay revealed no physical interaction between PHOT1 and 5PTase13 (see Supplemental Figure 3 online).

Deficiency of 5PTase13 Results in Increased $[Ca^{2+}]_{cyt}$

We hypothesize that inositol phosphate metabolism may provide a common link between 5PTase function and calcium fluctuations. It is generally believed that 5PTase13 functions in calcium signaling processes by regulating the level of Ins(1,4,5)P_3 and/or Ins(1,3,4,5)P_4, the two potent calcium-mobilizing molecules (Zhong et al., 2004; see Supplemental Figure 4 online). Indeed, our experiments indicated that Ins(1,4,5)P_3 and calcium levels appeared to be increased in the *5pt13* seedlings (Figure 5A; see Supplemental Figure 5 online).

To determine a possible connection between calcium levels and blue light responses in the *5pt13* mutant, we tested the effects of exogenous Ca^{2+} and its specific chelator EGTA on hypocotyl elongation. Whereas exogenous Ca^{2+} (10 to 20 mM) did not affect the hypocotyl lengths of the wild type or *5pt13* under blue light, this treatment resulted in shortened hypocotyls of *phot1*, *phot2*, and *phot1 phot2* mutants (see Supplemental Figure 6 online). The increased $[Ca^{2+}]_{cyt}$ in the *5pt13* mutant resulted in an altered responses to EGTA. In the hypocotyl assay, exogenous EGTA at low concentrations (100 μM) induced hypocotyl elongation in wild-type plants under blue light, especially under a higher fluence rate of blue light (35% longer, 20 μmol/m^2/s), and suppressed the elongation when higher concentrations (3 mM EGTA) were used (Figure 5B, top panel). However, *5pt13* mutant hypocotyls displayed reduced sensitivity to EGTA, and hypocotyl length was minimally affected by high concentrations of EGTA (Figure 5B, bottom panel).

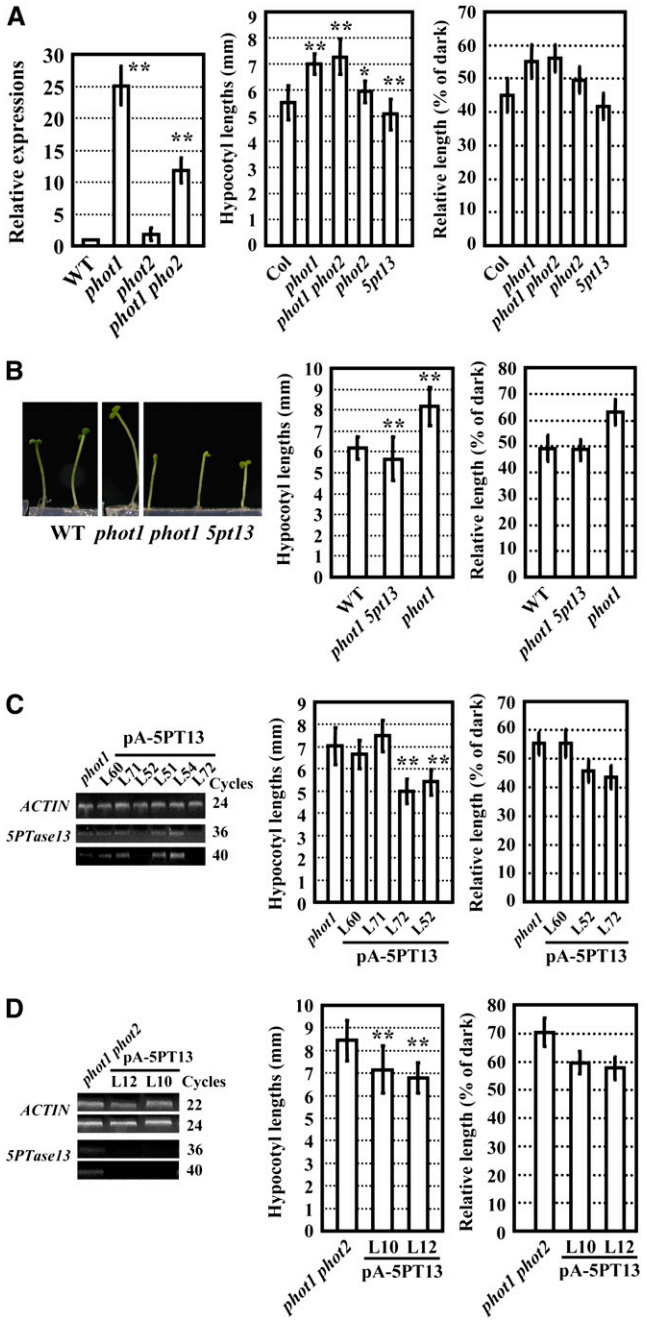

Figure 3. Deficiency of 5PTase13 Rescues the Shortened Hypocotyls of phot1.

(A) Quantitative real-time RT-PCR analysis showed that *5PTase13* transcriptions were enhanced in *phot1* and *phot1 phot2* but not in *phot2* seedlings under blue light (left panel; error bars represent SE of three independent replicates; **, $P < 0.01$). Compared with elongated hypocotyls of *phot1*, *phot2*, and *phot1 phot2* under blue light (20 μmol/m^2/s), *5pt13* had shortened hypocotyls (middle panel). Relative hypocotyl lengths, compared with that of dark-grown seedlings, are shown in the right panel. See Figure 1B for procedure and data presentation.

(B) Deficiency of *5PTase13* rescued the elongated hypocotyls of *phot1* under blue light (20 μmol/m^2/s; left panel). The lengths of hypocotyls were measured (middle panel), and the relative length was calculated (right panel).

(C) Suppressed expression of *5PTase13* in *phot1* as revealed by RT-PCR analysis (left panel) and correlated with shortened hypocotyls under blue light (20 μmol/m^2/s; middle panel). The relative length is shown in the right panel.

(D) RT-PCR analysis showing suppressed expression of *5PTase13* in *phot1 phot2* (left panel) correlated with shortened hypocotyls under blue light (20 μmol/m^2/s; middle panel). The relative length is shown in the right panel.

Further analysis showed that in the presence of a high concentration of EGTA (500 μM), the hypocotyl length of *5pt13* was also significantly increased under white light (a 1.5-fold increase; Figure 6A) and blue light (a 1.6-fold increase; Figure 6E) but not under red light, far-red light, or dark (Figures 6B to 6D). This result indicates that blue light and white light normally inhibit hypocotyl growth through increased $[Ca^{2+}]_{cyt}$; the addition of EGTA under these light conditions reduced calcium elevation, thereby promoting hypocotyl elongation. The observation that the *5pt13* mutant was less sensitive to a high concentration of EGTA (>2 mM) is consistent with the finding that *5PTase13* deficiency leads to an increased calcium elevation in the mutant.

To further test this idea, we also included the *phot1* and *phot2* mutants in the EGTA hypocotyl assay. Elongation of hypocotyls in the *phot1* and *phot2* single mutants and *phot1 phot2* double mutants, compared with that of *5pt13*, was not significantly altered by addition of exogenous EGTA (Figure 6E), further supporting the notion that increased $[Ca^{2+}]_{cyt}$ of *5pt13* may be a critical factor influencing the response of hypocotyls to blue light.

Previous studies have shown that *RPT2* transduces signals downstream of PHOT1 and is involved in the phototropic response and stomatal opening (Sakai et al., 2000; Inada et al., 2004). Indeed, analysis of gene expression profiling showed that *RPT2* transcript levels were enhanced significantly in *5pt13* seedlings (Table 1), further confirming that *5PTase13* is involved in phototropin signaling.

5PTase13 Regulates Blue Light Response by Increasing Ins(1,4,5)P_3 and $[Ca^{2+}]_{cyt}$

Our observation of increased calcium levels in the *5pt13* mutant and an earlier report on reduced calcium levels in the *phot1* mutant under blue light irradiation (Harada et al., 2003) suggest a possible link between *5PTase13* function and the *PHOT1* signaling pathways through the regulation of calcium signaling. We tested this idea by monitoring $[Ca^{2+}]_{cyt}$ changes under blue light irradiation using aequorin as a $[Ca^{2+}]_{cyt}$ indicator. Transgenic plants harboring cauliflower mosaic virus (CaMV) 35S promoter: aequorin were crossed with *5pt13*, *phot1*, or *5pt13 phot1* double mutants, and the offspring were analyzed by fluorescence imaging. Under blue light irradiation, the decay of aequorin luminescence took more time in *5pt13* seedlings (~45 s) compared with wild-type seedlings (~34 s) and *phot1* seedlings (only ~24 s), indicating a higher level of $[Ca^{2+}]_{cyt}$ in *5pt13* seedlings (the delayed time was calculated through comparison to seedlings

without CaMV35S:aequorin under the same irradiation situation). Furthermore, the decreased $[Ca^{2+}]_{cyt}$ in *phot1* seedlings was recovered in *5pt13 phot1* double mutants (Figure 7A, left panel). This is also consistent with the Ins(1,4,5)P_3 levels under blue light irradiation. As shown in Figure 7A (right panel), compared with

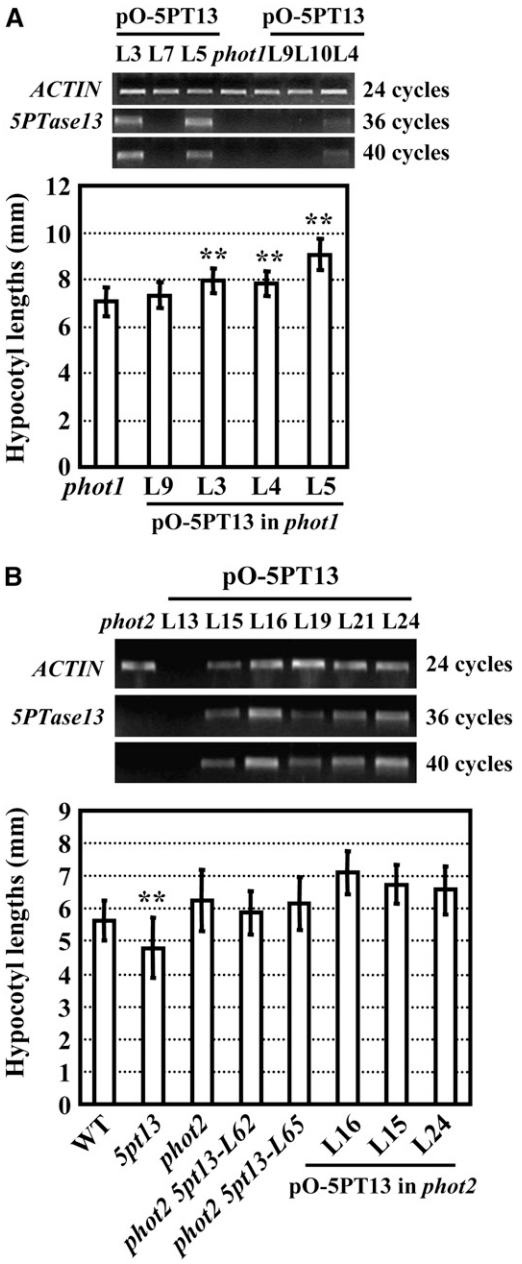

Figure 4. 5PTase13 Overexpression Enhances Hypocotyl Elongation of phot1 but Not phot2.

(A) Enhanced expression of *5PTase13* in *phot1* (top panel) resulted in elongated hypocotyls compared with *phot1* under blue light (bottom panel).
(B) Seedlings with deficiency of *5PTase13* in the *phot2* mutant background had similar hypocotyl length with *phot2* (bottom panel), and overexpression of *5PTase13* in *phot2* (top panel) did not result in shortened hypocotyl elongation under blue light (20 μmol/m^2/s; bottom panel).

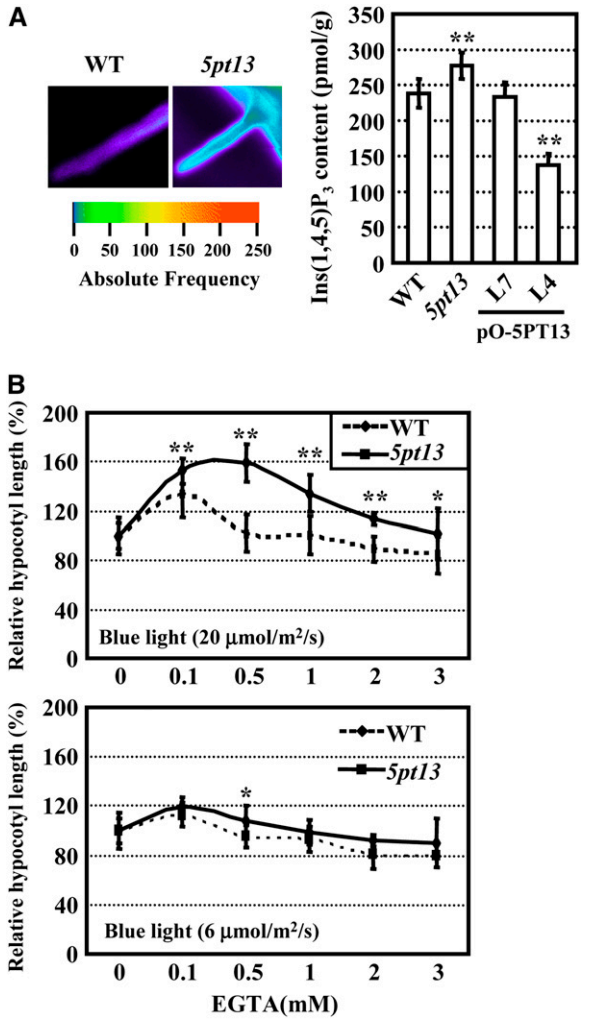

Figure 5. 5PTase13 Deficiency Results in Increased $[Ca^{2+}]_{cyt}$ and Renders Responses to Exogenous EGTA under Blue Light.

(A) $[Ca^{2+}]_{cyt}$ was increased in *5pt13* (left panel), consistent with the increased content of Ins(1,4,5)P_3 in *5pt13* (right panel). The Ins(1,4,5)P_3 content was reduced under overexpressed *5PTase13*. Image analysis was performed by UV confocal imaging. Root hairs were submerged with 20 μM Indo-1 and pseudocolor according to the cytoplasmic calcium levels. The data were representative of root hairs from >10 individual roots. Five-day-old seedlings grown on Murashige and Skoog (MS) medium under white light were used to measure the Ins(1,4,5)P_3 contents. Line 7 without overexpressed *5PTase13* after transformation (see Supplemental Figure 2A online) was used as a negative control. Assays were performed in triplicate, and the experiment was repeated two times and statistically analyzed using a one-tailed Student's *t* test ($P < 0.01$).
(B) *5pt13* had altered responses to exogenous EGTA under both high (top panel) and low (low panel) fluence rates of blue light. Hypocotyl lengths of 5-d-old seedlings were measured and statistically analyzed using a one-tailed Student's *t* test (*, $P < 0.05$; **, $P < 0.01$). Error bars represent SE ($n > 30$).

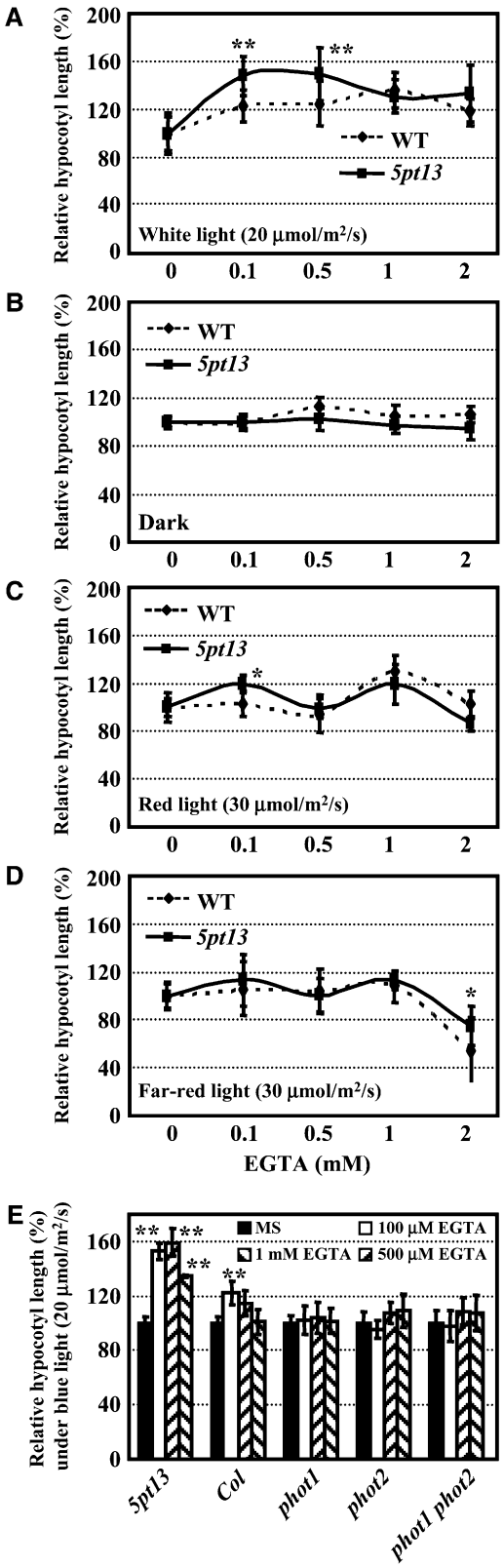

Figure 6. Responses of Hypocotyl Growth to EGTA under White Light and Blue Light.

Hypocotyl lengths of 5-d-old seedlings grown on the medium supplemented with EGTA under white light (60 μmol/m²/s; **[A]**), dark **(B)**, red light (30 μmol/m²/s; **[C]**) far-red light (30 μmol/m²/s; **[D]**), and blue light (20 μmol/m²/s; **[E]**) were measured and statistically analyzed using a Student's *t* test (*, $P < 0.05$; **, $P < 0.01$). Error bars represent SE ($n > 30$). Plant materials included wild-type, *5pt13*, *phot1*, *phot2*, and *phot1 phot2* seedlings.

the response under white light, Ins(1,4,5)P_3 levels decreased (~20%) under blue light in the wild type but were maintained at a higher level in the *5pt13* mutant. Accordingly, the Ins(1,4,5)P_3 levels in the *5pt13 phot1* double mutant were much higher than those in *phot1*.

In addition, seedlings overexpressing *5PTase13* appear to have reduced $[Ca^{2+}]_{cyt}$ under blue light (Figure 7B). These results indicate that *5PTase13* deficiency results in higher levels and longer durations of $[Ca^{2+}]_{cyt}$ elevation upon blue light irradiation, whereas *phot1* seedlings have lower levels and a shorter duration of $[Ca^{2+}]_{cyt}$ elevation relative to the wild type. We thus propose that *5PTase13* is involved in the blue light–stimulated increase in $[Ca^{2+}]_{cyt}$ and functions downstream of *PHOT1* in blue light signaling (Figure 7C).

DISCUSSION

Phosphatidylinositols regulate calcium fluctuations and other cellular functions. The 5PTases dephosphorylate Ins(1,4,5)P_3, Ins(1,3,4,5)P_4, or PtdIns(4,5)P_2, and often serve as terminators for calcium signaling. In this study, we show that *Arabidopsis 5PTase13* plays a role in the regulation of blue light responses. In particular, the expression of *5PTase13* was suppressed by blue light, whereas a deficiency of *5PTase13* resulted in a hypersensitive response to blue light in the hypocotyl assay. Disruption of *5PTase13* rescued the hypocotyl phenotype in the *phot1* mutant but not in the *cry1* mutant, indicating that 5PTase13 functions downstream of PHOT1 in blue light signaling. The *5pt13* mutant displayed enhanced $[Ca^{2+}]_{cyt}$, whereas *phot1* exhibited reduced $[Ca^{2+}]_{cyt}$ in response to blue light irradiation, leading to a model that PHOT1 suppresses 5PTase13 activity, thereby controlling calcium levels, which in turn regulate hypocotyl elongation.

Our study indicates that PHOT1 mediates blue light suppression of *5PTase13*, as this suppression was not evident in the *phot2* mutant. A previous study using microarray analysis (Ohgishi et al., 2004) showed that CRY1 and CRY2 appear to be the major receptors that mediate blue light–responsive gene expression, whereas PHOT1 and PHOT2 have very limited effects on the downstream light response genes. We speculate that the expression of some genes may have been altered in the *phot1* and *phot2* mutants in the microarray study, although such change may be relatively small compared with changes in the *cry1* and *cry2* mutants. We noted that Ohgishi et al. (2004) used 11-d-old seedlings, whereas 4-d-old seedlings were used in our studies. Along the line of differential function by CRY and PHOT family receptors, it is well documented that CRY proteins plays a major role in hypocotyl growth and PHOT proteins functions in phototropism, chloroplast orientation, and stomatal opening. We speculate that the contribution of PHOT1 to the regulation of

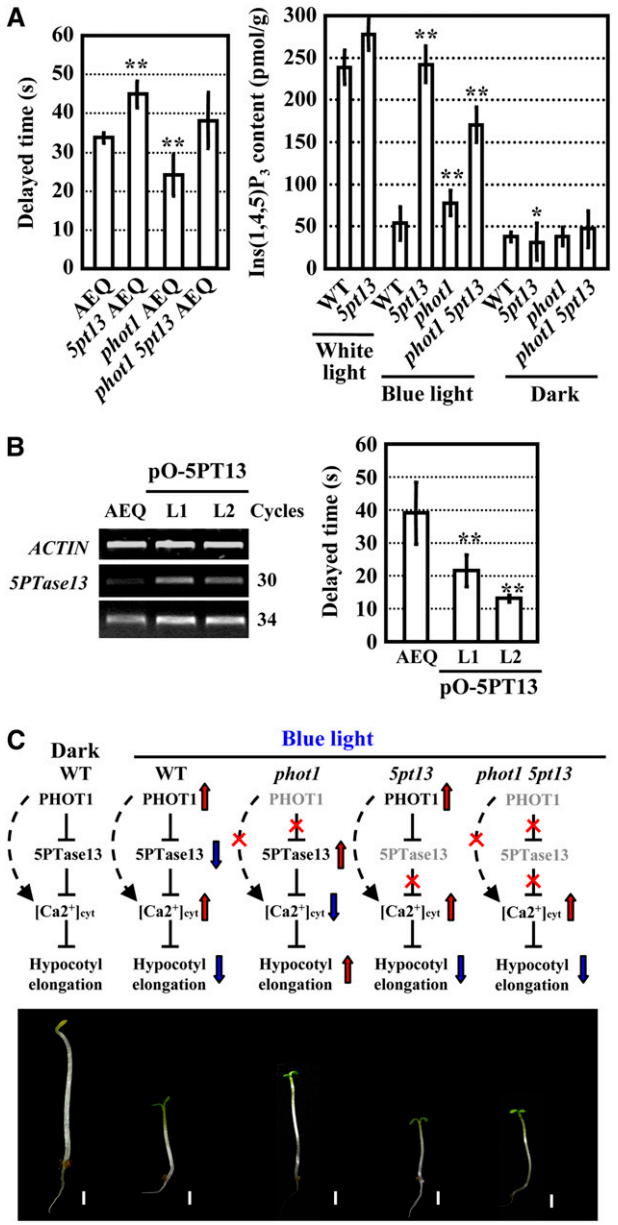

Figure 7. 5PTase13 Functions in the Blue Light–Stimulated $[Ca^{2+}]_{cyt}$ Increase.

(A) *5pt13* had enhanced $[Ca^{2+}]_{cyt}$ (left panel) and increased Ins(1,4,5)P_3 levels (right panel) under blue light irradiation compared with the wild-type control. The data were statistically analyzed using a Student's *t* test (*, $P < 0.05$; **, $P < 0.01$). Error bars represent SE ($n > 20$).

(B) Enhanced expression of *5PTase13* resulted in reduced $[Ca^{2+}]_{cyt}$ under blue light irradiation. The data were statistically analyzed using a one-tailed Student's *t* test (**, $P < 0.01$). Error bars represent SE ($n > 20$).

(C) Hypothetical model depicting 5PTase13 function in the blue light–mediated $Ca^{2+}_{[cyt]}$ increase and hypocotyl growth inhibition.

hypocotyl growth is less significant compared with the other photoreceptors, such as CRY1, and may explain why *5pt13* mutants displayed a rather subtle hypocotyl growth phenotype. The changes in hypocotyl length in both *5pt13* and *phot1* mutants were statistically significant, although small. Furthermore, a deficiency of *5PTase13* in *phot1* mutant seedlings rescues the hypocotyl phenotype and causes changes in calcium levels, suggesting that crosstalk between *5PTase13* and *PHOT1* plays a role in blue light responses.

Much effort has been focused on the identification of signaling components downstream of blue light receptors and upstream of phenotypic effects, such as inhibition of hypocotyl growth. Several studies have shown that blue light induces elevation of $[Ca^{2+}]_{cyt}$, and mutations in genes encoding blue light receptors, such as PHOT1 or PHOT2, have compromised calcium elevation, leading to changes in photomorphogenesis (Babourina et al., 2002; Harada et al., 2003; Stoelzle et al., 2003). It is interesting to note that defects in PHOT1 and $[Ca^{2+}]_{cyt}$ appear to affect only the short term initial phase of the hypocotyl growth response, and further inhibition of hypocotyl elongation requires the CRY1-COP1 pathway (Parks et al., 1998; Folta and Spalding, 2001). Our study addresses a missing link between the photoreceptors and the calcium second messenger. More specifically, we identified *5PTase13* as a component that regulates calcium signals in the *PHOT1* pathway.

How does *PHOT1* regulate the activity of *5PTase13*? Our study provides evidence that *5PTase13* is regulated by blue light through *PHOT1*, at least in part, at the transcriptional level. Our quantitative RT-PCR analysis indicated that *5PTase13* mRNA levels were downregulated by blue light. The finding that the *5PTase13* promoter-GUS reporter negatively responds to blue light confirmed the notion that regulation occurred at the level of transcription. However, we cannot exclude the possibility that *5PTase13* also might be regulated by *PHOT1* through other mechanisms, such as direct modification of enzyme activity. The protein–protein interaction by yeast two-hybrid assay did not detect a physical interaction between PHOT1 and 5PTase13 (see Supplemental Figure 3B online); however, the kinase–substrate interaction was often weak and transient, and further studies are needed to determine if 5PTase13 is in fact a substrate of PHOT1.

Blue light suppression of *5PTase13* reveals a double-negative step in blue light signaling, and such negative-negative regulation steps appear to be a common feature of plant signal transduction. For example, similar double-negative steps are found in ethylene signal transduction where ethylene receptors negatively regulate the downstream CONSTITUTIVE TRIPLE RESPONSE1 kinase, which in turn inhibits ethylene responses (Stepanova and Alonso, 2005). We propose that under darkness, the protein level (and activity) of 5PTase13 is high, keeping $[Ca^{2+}]_{cyt}$ low, and hypocotyls elongate rapidly. Upon light irradiation, PHOT1 is activated, leading to suppression of 5PTase13, and an elevation of cytosolic calcium takes place resulting in inhibition of hypocotyl growth.

Several major questions remain to be addressed, including how 5PTase13 regulates calcium, and what the function of calcium is in cell elongation. While little information is available regarding calcium action in cell growth upon blue light irradiation, previous studies have built a connection between 5PTase13 and

calcium fluctuations in the cell. At least several inositol phosphates molecules, especially Ins(1,4,5)P_3 and Ins(1,3,4,5)P_4, have been shown to mediate calcium fluxes across cell membranes. Such transport processes can include release of calcium from intracellular stores or influxes from the apoplast through inward calcium channels. Intracellular calcium is stored in the vacuole, which harbors ligand-gated calcium channels or Ins(1,4,5)P_3 receptors. High levels of Ins(1,4,5)P_3 activate these calcium channels and then release calcium to the cytosol. The phosphate group at the 5′ position of the inositol ring is thought to be important for ligand specificity of calcium channels, and dephosphorylation at the 5′ position by 5PTases could reduce the level of active ligands, leading to the closure of calcium channels and termination of the signaling process. Therefore, the 5PTases function as terminators for calcium signaling, which might be initiated by various signals, including blue light, as demonstrated here. In this context, earlier studies have identified both plasma membrane channels and intracellular calcium stores that are involved in blue light signaling (Harada et al., 2003; Stoelzle et al., 2003). However, the molecular nature of these channels remains elusive. Toward a better understanding of calcium channels involved in blue light signaling, further identification of 5PTase13 substrates would provide clues about the ligands that activate the calcium channels. Our results constitute substantial progress toward this goal: Ins(1,4,5)P_3 levels appear to fluctuate consistently with calcium levels, suggesting the possibility that the Ins(1,4,5)P_3 receptor could be the calcium release channel involved in blue light responses. How might $[Ca^{2+}]_{cyt}$ mediate cell elongation? A simple interpretation is that blue light induces Ca^{2+} and H^+ fluxes (Babourina et al., 2002), both of which are critical for cell growth.

5PTase13 expression was similarly suppressed by both blue and red light compared with darkness. However, *5pt13* mutants exhibited shortened hypocotyls and larger cotyledons under blue light but smaller cotyledons under red light (Figure 1C). The phytochrome A–specific signaling intermediate *SPA1* (Hoecker and Quail, 2001; Laubinger et al., 2004) was significantly upregulated under *5PTase13* deficiency, suggesting that *5PTase13* might participate in other light-mediated growth processes or signaling pathways in addition to playing a major role in blue light signaling.

METHODS

Plant Growth and Light Conditions

Arabidopsis thaliana (Columbia ecotype) seeds were surface sterilized with 20% bleach for 15 min and washed four times with sterile water and planted aseptically on agar medium containing Murashige and Skoog (1962) salts and 2% sucrose (w/v). In some cases, the medium was supplemented with 25 μg/mL of hygromycin, 15 μg/mL of basta, or 25 μg/mL of kanamycin to screen the resistant transgenic plants or homozygous mutants. After 48 h of vernalization, seedlings were grown at 22°C with a 16-h-white light/8-h-dark cycle, followed by continued growth under the same conditions or transfer to blue light, red light- or far-red light (continuous light) with different fluence rates for 5 d. Exogenous EGTA or calcium treatment was performed by growing the seedlings on MS medium supplemented with different concentrations of EGTA or calcium chloride for 5 d.

All experiments involving blue light, red light, or far-red light illumination were performed in an E-30 LED chamber (Percival) using the blue diodes (λmax = 469 nm), red diodes (λmax = 680 nm), or far-red light (λmax = 730 nm) at 22°C in continuous light. Light fluence rates were measured using an Li250 quantum photometer (Li-Cor).

Hypocotyl length and cotyledon area were measured using the E-ruler software and statistically analyzed. Photos were taken by an SMZ 800 stereoscope (Nikon) equipped with a Nikon digital Coolpix 995 camera. Statistical analyses were performed using Excel tools as described in the figure legends. All experiments were performed in triplicate ($n > 30$).

Mutant Confirmation and Plant Crosses

The *5pt13* mutant obtained from Syngenta (Garlic 350-F1; http://www.syngenta.com) carried a T-DNA insertion in the fourth exon (Lin et al., 2005). Double mutants were produced by the standard method previously described (Weigel and Glazebrook, 2002). Offspring of the double mutant were analyzed by PCR amplifications with primers 5pt13-1 (5′-TCCGAACGGAATTGTCTCAG-3′) and 5pt13-2 (5′-GCAACATCAAGATCTCCAACA-3′), phot1-s (5′-TCCACTTGCAACCTATGCGTG-3′) and phot1-a (5′-ACCGCTTCATCGATATTCACA-3′), phot2-s (5′-ATGGAGAGGCCAAGAGCCC-3′) and phot2-a (5′-TGTCGGTGTCTGGCCCTTGC-3′) (Mao et al., 2005), cry1-s (5′-GGGAGAGATGTCTTAGTATGCCTTATG-3′) and cry1-a (5′-CCCCTCGAGCCCGGTTTGTGAAAGCCGTCT-3′) (Bruggemann et al., 1996), and aequorin-s (5′-ATGACAAGCAAACAATACTCAGT-3′) and aequorin-a (5′-TTAGGGGACAGCTCCACCG-3′). PCR analysis of the heterozygous *phot1*/+, *phot2*/+, *cry1*/+ *cop1*/+, and homozygous *phot1 phot2* and *cry1 cop1* plants was performed as described earlier (Mao et al., 2005; Sang et al., 2005).

GUS Histochemical Staining

Transgenic seedlings harboring a *5PTase13* promoter-GUS reporter gene construct were stained at 37°C overnight in a solution of 5-bromo-4-chloro-3-indolyl-β-D-glucuronic acid (final concentration 1 mg/mL), potassium ferricyanide (final concentration 0.5 mM), potassium ferrocyanide (final concentration 0.5 mM), 0.1% Triton X-100 (final concentration 0.1% [v/v]), and sodium phosphate buffer (final concentration 0.1 M), pH 7.0 (Rook et al., 1998).

Yeast Two-Hybrid Analysis

The cDNA fragment for the complete WD40 repeats of 5PTase13 was amplified by primers 5pt13-11 (5′-CATGCCATGGTATGAGGCTGGGTGTGGGATTG-3′; *Nco*I site underlined) and 5pt13-12 (5′-CCGCTCGAGGCTTGAAATTAGCTTTCCGTC-3′; *Xho*I site underlined), and the fragment containing N-terminal and WD40 repeats, designated as N-WD, was amplified by primers 5pt13-13 (5′-CATGCCATGGCGATGGATTCGCTAATTATCG-3′; *Nco*I site underlined) and 5pt13-12. Resulting fragments were subcloned into the pEG202 vector and confirmed by restriction enzyme digestion and DNA sequencing. Other constructs harboring DNA fragments encoding GUS, *Arabidopsis* CRY1 C-terminal domain (CCT1), CRY1, or COP1 in pJG4-5 were kindly provided by Hong-Quan Yang (Yang et al., 2001). All combinations of prey and bait constructs were cotransformed into the yeast strain EGY48 through the standard ONE-STEP method (Chen et al., 1992).

The DNA fragment encoding N-terminal and WD40 repeats of 5PTase13 was amplified by primers 5pt13-14 (5′-CGCGGATCCCGATGGATTCGCTAATTATC-3′; *Bam*HI site underlined) and 5pt13-15 (5′-ACGCGTCGACGGGTCCTGGAGATGTCAC-3′; *Sal*I site underlined) and that encoding the 5PTase13 catalytic domain was amplified by primers 5pt13-16 (5′-GGACAACATAATCCGAACGGA-3′) and 5pt13-17 (5′-ACGCGTCGACTCTCGAGTGTCTTCGCACC-3′; *Sal*I site underlined). Resulting fragments were cloned into the pGBKT7 vector and confirmed by restriction enzyme digestion and DNA sequencing. The DNA fragment

encoding the LOV domain of PHOT1 was amplified by primers PHOT1-l1 (5′-CGGAATTCATGGAACCAACAGAAAAACCA-3′; *Eco*RI site underlined) and PHOT1-l2 (5′-CGGGATCCTGGTGTCATGTTGGCATCAG-3′; *Bam*HI site underlined) and that encoding the PHOT1 kinase domain was amplified by primers PHOT1-k1 (5′-CGGAATTCGAGGATTTATGGGCAAACCA-3′; *Eco*RI site underlined) and PHOT1-k2 (5′-CGGGATCCAACATTTGTTTGCAGATCTTCT-3′; *Bam*HI site underlined). Resulting fragments were cloned into the pGADT7 vector and confirmed by restriction enzyme digestion and DNA sequencing. All combinations of prey and bait constructs were cotransformed into the yeast strain AH109 through the small-scale LiAc yeast transformation method (Clontech).

Interaction analysis, including growth marker-based selection and measurement of the β-galactosidase activity, were essentially performed as described previously (McNellis et al., 1996) or according to the manufacturer's manual (Matchmaker LexA two-hybrid system; Clontech).

Coimmunoprecipitation Analysis

Coimmunoprecipitation was performed using extracts prepared from yeast cells, as described by Nam and Li (2002). The protease inhibitor cocktail (Sigma-Aldrich), anti-MYC monoclonal antibody (NeoMarkers), anti-HA polyclonal antibody (NeoMarkers), nitrocellulose membrane (Schleicher and Schuell), and a nitroblue tetrazolium/bromochloroindolyl phosphate system were used during the process as previously described (Lou et al., 2007).

Constructs and Plant Transformation

Primers 5pt13-3 (5′-ACGCGTCGACCATGGATTCGCTAATTATCGAAG-3′; *Sal*I site underlined) and 5pt13-4 (5′-GGACTAGTTCTCGAGTGTCTTCGCACC-3′; *Spe*I site underlined) were used to amplify the full-length cDNA of *5PTase13*. The resulting 3300-bp cDNA was cloned into the pCAMBIA1302 vector in the sense orientation to generate the overexpression construct. The antisense vector was generated with a 600-bp coding region at the 5′-end of *5PTase13* cDNA, which was amplified by primers 5pt13-5 (5′-ATGGATTCGCTAATTATCG-3′) and 5pt13-6 (5′-GAAGTAGTAACAGACTCATG-3′). This cDNA region was first cloned into the PMD18-T vector and then subcloned into the PHB vector in the antisense orientation. The *5PTase13* promoter was amplified by primers 5pt13-P-1 (5′-ACGCGTCGACACCATCTTGGGTCGTTAATTAGTT-3′; *Sal*I site underlined) and 5pt13-P-2 (5′-CGCGGATCCCGACAATCAGAGGAATTCAAG-3′; *Bam*HI site underlined). The resulting 1.0-kb fragment was cloned into the p1300 vector and confirmed by restriction enzyme digestion. The constructs were transferred into *Agrobacterium tumefaciens* strain GV3101 and transformed into *Arabidopsis* plants (Columbia ecotype) by the floral dip method (Weigel and Glazebrook, 2002).

RT-PCR and Quantitative Real-Time PCR Analysis

Total RNA was extracted from open flowers or seedlings (grown in a 16-h-white light/8-h-dark cycle) using TRIzol reagent (Invitrogen) and used for RT-PCR analysis. The cDNA was produced by reverse transcription with oligo(dT) (ReverTra Ace-α-first-strand synthesis kit; Toyobo), and PCR amplification was performed by specific primers 5pt13-7 (5′-TCCGAACGGAATTGTCTCAG-3′) and 5pt13-8 (5′-GCAACATCAAGATCTCCAACA-3′). The *Arabidopsis* ACTIN8 gene, amplified by primers actin-1 (5′-GATGCTGATGACATTCAACCT-3′) and actin-2 (5′-GAAGTGAGAAACCCTCATAG-3′), was used as a positive internal control.

Quantitative real-time RT-PCR analysis was performed with the RotorGene 3000 (Corbett Research) using a SYBR green detection protocol (SYBR Premix Ex Taq System; TaKaRa). The product amounts were determined by the method of comparative Δ-Δ Ct. (Fleige et al., 2006). The primers used for *5PTase13* were 5pt13-9 (5′-CCGAGGACAAAATCTAAGTAACG-3′) and 5pt13-10 (5′-CAGCGCCGGTGCTTGGAATAG-3′). *Arabidopsis ACTIN7* was amplified by primers actin-3 (5′-CCGGTATTGTGCTCGATTCTG-3′) and actin-4 (5′-TTCCCGTTCTGCGGTAGTGG-3′) and used as internal positive control. The experiments were repeated more than three times.

Measurement of $[Ca^{2+}]_{cyt}$

$[Ca^{2+}]_{cyt}$ was measured in vivo by luminometry using intact seedlings expressing aequorin as described previously (Harada et al., 2003; Love et al., 2004; Plieth, 2006). Seedlings were grown under a 16-h-white light/8-h-dark cycle for 10 days and clusters of three plants floated in the 200 μL solution containing coelenterazine (final concentration at 1 μM) free base (Sigma-Aldrich) in the dark overnight. The measurements were performed in the luminometer cuvette (2 mL) containing coelenterazine (1 μM)-free base. The reading began after giving a 20-s blue light (20 μmol/m^2/s) pulse in the luminometer (FG-200) (Wang and Gu, 1986; Demidchik et al., 2004; Hu et al., 2004; Love et al., 2004). Fluorescence was generated by the sum of autofluorescence of chlorophyll and aequorin luminescence. To detect aequorin fluorescence, the time difference was calculated by comparison to seedlings without CaMV35S:aequorin under the same irradiation situation, which was termed as "delayed time."

Fluorescence imaging of $[Ca^{2+}]_{cyt}$ was performed according to Legue et al. (1997) and Wymer et al. (1997). Briefly, seedlings were floated in Indo-1 solution (20 μM; in 10 mM dimethylglutaric acid, pH 4.5) and incubated in the dark for 1 h. After washing with liquid MS medium, seedlings were placed on a Zeiss inverted microscope (LSM510 META) for fluorescence imaging (364-nm excision and 400- to 435-nm and 480 ± 20-nm emission). The distribution of Ca^{2+} was imaged from the root hair or root tip. Calcium levels were pseudocolored according to the scale.

Measurement of Ins(1,4,5)P_3 Content

Five-day-old seedlings grown on MS medium under dark, white light, or blue light (20 μmol/m^2/s) were used for the measurement of Ins(1,4,5)P_3 contents. Three hundred milligrams of freshly ground tissue was used for extraction of Ins(1,4,5)P_3 according to the procedure described by Burnette et al. (2003). Ins(1,4,5)P_3 content was measured using the D-myo-inositol-1,4,5-trisphosphate [^{3}H] assay kit (Amersham-Pharmacia Biotech). The Ins(1,4,5)P_3 content in the samples was interpolated from a standard curve generated with known amounts of Ins(1,4,5)P_3. Assays were performed in triplicate, and the experiment was repeated two times.

Expression, Purification, and Biochemical Characterization of Recombinant 5PTase13

Expression of recombinant 5PTase13 in *Escherichia coli* cells was performed according to Sanchez and Chua (2001). Briefly, the full-length *5PTase13*-encoding sequence was N-terminally fused to a polyhistidine-tag and a T7-tag and expressed in *E. coli* cells according to the supplier's instructions (Gibco BRL). To generate the plasmid pET28b-5PTase13, a DNA fragment encompassing the entire *5PTase13* cDNA was PCR amplified using primers 5pt13-18 (5′-ACGCGTCGAC*ATG*GATTCGCTAATTATCGAAG-3′; added *Sal*I site underlined and the start ATG site in italics) and 5pt13-19 (5′-GGGACGATGCGGCCGCTATATCTCGAGTGTC-3′; added *Not*I site underlined) and subcloned into the pET28b vector (Novagen). The in-frame reading of the construct was confirmed by sequencing to avoid nucleotide substitutions during PCR amplification. Transformed *E. coli* cells harboring pET28b-5PTase13 were cultured at 37°C, and protein expression was induced by 1 mM isopropylthio-β-galactoside (final concentration) for 8 h. Cells were then harvested, resuspended in lysis buffer (50 mM NaH_2PO_4, 300 mM NaCl, and 250 mM

imidazol), and sonicated. The resulting supernatants (lysates) were purified on His-tag beads (Sigma-Aldrich), and the purified proteins were analyzed by SDS-PAGE and protein gel blotting with a T7 monoclonal antibody (Novagen). Recombinant 5PTase13 catalytic domain protein was expressed and purified using a similar procedure, employing vector pET28a and primers 5pt13-20 (5′-CGGGGATCCAAGGAAACTTTATATGCCAG-3′; added *Bam*HI site underlined) and 5pt13-21 (5′-CGGCTCGAGTCACAGATTTATCAACATGAG-3′; added *Xho*I site underlined).

Enzymatic analyses were performed by incubation of purified protein (1.5 μg) at 37°C overnight in solutions containing 50 mM Tris-HCl, pH 7.4, 100 mM NaCl, and 2 mM $MgCl_2$, supplemented with either 20 mM Ins(1,4,5)P_3 and 0.02 μCi [^{3}H]Ins(1,4,5)P_3 (10 mM), or 20 mM Ins(1,3,4,5)P_4 and 0.016 μCi [^{3}H]Ins(1,3,4,5)P_4 (10 mM). The reactions were terminated by heating at 95°C for 5 min (Sanchez and Chua, 2001), and HPLC analysis was performed as described (Xue et al., 1999).

Microarray Hybridization and Analysis

The microarray hybridization using the *Arabidopsis* ATH1 chip was described by Lin et al. (2005). Briefly, the aerial organs of 4-d-old wild-type and *5pt13* seedlings grown in continuous white light were used for RNA extraction. Furthermore, 15 μg of purified biotin-labeled copy RNA, which was fragmented into 35 to 300 nucleotides, was used for microarray analysis. Two hybridizations (independent biological replicates) were performed for each genotype (wild type or *5pt13*) for a total of four hybridizations. Arrays were scanned with the Agilent GeneArray scanner (Affymetrix), and the obtained data were normalized with the Affymetrix Microarray Suite program (version 5.0) and set the algorithm absolute call flag according to P (present), M (marginal), and A (absent). The data were then imported into R software (http://www.R-project.org) and analyzed using the robust test statistics described in the Limma package (Smyth, 2005). The data exhibited intensity-dependent biases; therefore, $\log_2(X)$ ($X =$ scaling signal) transformed data were further corrected with a global Lowess transformation. FDRs for various P value thresholds were determined by the method of Benjamini and Yekutieli (2001).

Accession Numbers

Sequence data from this article can be found in the GenBank/EMBL data libraries under the following accession numbers: *5PTase13* (At1g05630, AJ297426), *CRY1* (At4g08920, NM_116961), *COP1* (At2g32950, NM_128855), *Actin7* (At5g09810, NM_121018), *Actin8* (At1g49240, NM_103814), *PHOT1* (At3g45780, NM_114447), and *PHOT2* (At5g58140, NM_125199).

Supplemental Data

The following materials are available in the online version of this article.

Supplemental Figure 1. Histochemical Staining of 5PTase13 Promoter: GUS-Containing Seedlings.

Supplemental Figure 2. Overexpression of 5PTase13 in 5pt13 or Wild-Type Plants, as Revealed by RT-PCR Analysis.

Supplemental Figure 3. 5PTase13 Does Not Interact with PHOT1 Protein.

Supplemental Figure 4. 5PTase13 Deficiency Results in Increased $[Ca^{2+}]_{cyt}$ under White Light.

Supplemental Figure 5. The 5PTase13 Protein Exhibits Phosphatase Activities toward Ins(1,3,4,5)P_4.

Supplemental Figure 6. Responses of Hypocotyl Growth to Calcium under Blue Light.

ACKNOWLEDGMENTS

This work was supported by the National Natural Science Foundation of China (Grants 30425029 and 30421001), by the Shanghai municipal government (Grant 055407072), and by a grant from the National Science Foundation (to S.L.). We thank Hong-Quan Yang (Institute of Plant Physiology and Ecology, Chinese Academy of Sciences) for providing seeds of *phot1*, *phot2*, *phot1 phot2*, *cry1*, and *cop1*. We also thank Alex A.R. Webb and Mark Tester (University of Cambridge, Cambridge, UK) for the gifts of Wassilewskija ecotype and Columbia ecotype harboring CaMV35S:aequorin and Jian-Ben Gu (Institute of Plant Physiology and Ecology, Chinese Academy of Sciences) for the luminometer measurement of $[Ca^{2+}]_{cyt}$.

Received May 5, 2007; revised November 22, 2007; accepted January 21, 2008; published February 5, 2008.

REFERENCES

Ang, L.H., Chattopadhyay, S., Wei, N., Oyama, T., Batschauer, A., and Deng, X.W. (1998). Molecular interaction between COP1 and HY5 defines a regulatory switch for light control of Arabidopsis development. Mol. Cell **1:** 213–222.

Babourina, O., Newman, I., and Shabala, S. (2002). Blue light-induced kinetics of H^+ and Ca^{2+} fluxes in etiolated wild-type and phototropin-mutant Arabidopsis seedlings. Proc. Natl. Acad. Sci. USA **99:** 2433–2438.

Baum, G., Long, J.C., Jenkins, G.I., and Trewavas, A.J. (1999). Stimulation of the blue light phototropic receptor NPH1 causes a transient increase in cytosolic Ca^{2+}. Proc. Natl. Acad. Sci. USA **96:** 13554–13559.

Benjamini, Y., and Yekutieli, D. (2001). The control of the false discovery rate in multiple testing under dependency. Ann. Statist. **29:** 1165–1188.

Berdy, S.E., Kudla, J., Gruissem, W., and Gillaspy, G.E. (2001). Molecular characterization of At5PTase1, an inositol phosphatase capable of terminating inositol trisphosphate signaling. Plant Physiol. **126:** 801–810.

Briggs, W.R. (2007). The LOV domain: A chromophore module servicing multiple photoreceptors. J. Biomed. Sci. **14:** 499–504.

Briggs, W.R., and Christie, J.M. (2002). Phototropins 1 and 2: Versatile plant blue-light receptors. Trends Plant Sci. **7:** 204–210.

Bruggemann, E., Handwerger, K., Essex, C., and Storz, G. (1996). Analysis of fast neutron-generated mutants at the *Arabidopsis thaliana* HY4 locus. Plant J. **10:** 755–760.

Burnette, R.N., Gunesekera, B.M., and Gillaspy, G.E. (2003). An Arabidopsis inositol 5-phosphatase gain-of-function alters abscisic acid signaling. Plant Physiol. **132:** 1011–1019.

Carland, F.M., and Nelson, T. (2004). Cotyledon vascular pattern2-mediated inositol (1,4,5) trisphosphate signal transduction is essential for closed venation patterns of *Arabidopsis* foliar organs. Plant Cell **16:** 1263–1275.

Casazza, A.P., Rossini, S., Rosso, M.G., and Soave, C. (2005). Mutational and expression analysis of ELIP1 and ELIP2 in *Arabidopsis thaliana.* Plant Mol. Biol. **58:** 41–51.

Chen, D.C., Yang, B.C., and Kuo, T.T. (1992). One-step transformation of yeast in stationary phase. Curr. Genet. **21:** 83–84.

Cho, H.Y., Tseng, T.S., Kaiserli, E., Sullivan, S., Christie, J.M., and Briggs, W.R. (2007). Physiological roles of the light, oxygen, or voltage domains of phototropin 1 and phototropin 2 in *Arabidopsis.* Plant Physiol. **143:** 517–529.

Cho, M.H., and Spalding, E.P. (1996). An anion channel in *Arabidopsis* hypocotyls activated by blue light. Proc. Natl. Acad. Sci. USA **93:** 8134–8138.

Christie, J.M. (2007). Phototropin blue-light receptors. Annu. Rev. Plant Biol. **58:** 21–45.

Cosgrove, D.J. (2005). Growth of the plant cell wall. Nat. Rev. Mol. Cell Biol. **6:** 850–861.

Demidchik, V., Essah, P.A., and Tester, M. (2004). Glutamate activates cation currents in the plasma membrane of *Arabidopsis* root cells. Planta **219:** 167–175.

Du, L., and Poovaiah, B.W. (2005). Ca^{2+}/calmodulin is critical for brassinosteroid biosynthesis and plant growth. Nature **437:** 741–745.

Emi, T., Kinoshita, T., Sakamoto, K., Mineyuki, Y., and Shimazaki, K. (2005). Isolation of a protein interacting with Vfphot1a in guard cells of *Vicia faba.* Plant Physiol. **138:** 1615–1626.

Fleige, S., Walf, V., Huch, S., Prgomet, C., Sehm, J., and Pfaffl, M.W. (2006). Comparison of relative mRNA quantification models and the impact of RNA integrity in quantitative real-time RT-PCR. Biotechnol. Lett. **28:** 1601–1613.

Folta, K.M., Lieg, E.J., Durham, T., and Spalding, E.P. (2003). Primary inhibition of hypocotyl growth and phototropism depend differently on phototropin-mediated increases in cytoplasmic calcium induced by blue light. Plant Physiol. **133:** 1464–1470.

Folta, K.M., and Spalding, E.P. (2001). Unexpected roles for cryptochrome2 and phototropin revealed by high-resolution analysis of blue light-mediated hypocotyl growth inhibition. Plant J. **26:** 471–478.

Franklin, K.A., Larner, V.S., and Whitelam, G.C. (2005). The signal transducing photoreceptors of plants. Int. J. Dev. Biol. **49:** 653–664.

Gunesekera, B., Torabinejad, J., Robinson, J., and Gillaspy, G.E. (2007). Inositol polyphosphate 5-phosphatases 1 and 2 are required for regulating seedling growth. Plant Physiol. **143:** 1408–1417.

Guo, H., Mockler, T., Duong, H., and Lin, C. (2001). SUB1, an Arabidopsis Ca^{2+}-binding protein involved in cryptochrome and phytochrome coaction. Science **291:** 487–490.

Harada, A., Sakai, T., and Okada, K. (2003). Phot1 and phot2 mediate blue light-induced transient increases in cytosolic Ca^{2+} differently in *Arabidopsis* leaves. Proc. Natl. Acad. Sci. USA **100:** 8583–8588.

Harada, A., and Shimazaki, K. (2007). Phototropins and blue light-dependent calcium signaling in higher plants. Photochem. Photobiol. **83:** 102–111.

Hoecker, U., and Quail, P.H. (2001). The phytochrome A-specific signaling intermediate SPA1 interacts directly with COP1, a constitutive repressor of light signaling in *Arabidopsis.* J. Biol. Chem. **276:** 38173–38178.

Hu, X.Y., Neill, S.J., Cai, W.M., and Tang, Z.C. (2004). Induction of defence gene expression by oligogalacturonic acid requires increases in both cytosolic calcium and hydrogen peroxide in *Arabidopsis thaliana.* Cell Res. **14:** 234–240.

Inada, S., Ohgishi, M., Mayama, T., Okada, K., and Sakai, T. (2004). RPT2 is a signal transducer involved in phototropic response and stomatal opening by association with phototropin 1 in *Arabidopsis thaliana.* Plant Cell **16:** 887–896.

Jones, M.A., Raymond, M.J., and Smirnoff, N. (2006). Analysis of the root-hair morphogenesis transcriptome reveals the molecular identity of six genes with roles in root-hair development in *Arabidopsis.* Plant J. **45:** 83–100.

Kasahara, M., et al. (2002). Photochemical properties of the flavin mononucleotide-binding domains of the phototropins from *Arabidopsis*, rice, and *Chlamydomonas reinhardtii.* Plant Physiol. **129:** 762–773.

Kim, J.I., Park, J.E., Zarate, X., and Song, P.S. (2005). Phytochrome phosphorylation in plant light signaling. Photochem. Photobiol. Sci. **4:** 681–687.

Kimura, M., and Kagawa, T. (2006). Phototropin and light-signaling in phototropism. Curr. Opin. Plant Biol. **9:** 503–508.

Kinoshita, T., Emi, T., Tominaga, M., Sakamoto, K., Shigenaga, A., Doi, M., and Shimazaki, K. (2003). Blue-light- and phosphorylation-dependent binding of a 14-3-3 protein to phototropins in stomatal guard cells of broad bean. Plant Physiol. **133:** 1453–1463.

Lariguet, P., Schepens, I., Hodgson, D., Pedmale, U.V., Trevisan, M., Kami, C., de Carbonnel, M., Alonso, J.M., Ecker, J.R., Liscum, E., and Fankhauser, C. (2006). PHYTOCHROME KINASE SUBSTRATE 1 is a phototropin 1 binding protein required for phototropism. Proc. Natl. Acad. Sci. USA **103:** 10134–10139.

Lascève, G., Leymarie, J., Olney, M.A., Liscum, E., Christie, J.M., Vavasseur, A., and Briggs, W.R. (1999). *Arabidopsis* contains at least four independent blue-light-activated signal transduction pathways. Plant Physiol. **120:** 605–614.

Laubinger, S., Fittinghoff, K., and Hoecker, U. (2004). The SPA quartet: A family of WD-repeat proteins with a central role in suppression of photomorphogenesis in *arabidopsis.* Plant Cell **16:** 2293–2306.

Legue, V., Blancaflor, E., Wymer, C., Perbal, G., Fantin, D., and Gilroy, S. (1997). Cytoplasmic free Ca^{2+} in Arabidopsis roots changes in response to touch but not gravity. Plant Physiol. **114:** 789–800.

Li, Q.H., and Yang, H.Q. (2007). Cryptochrome signaling in plants. Photochem. Photobiol. **83:** 94–101.

Lin, C., and Todo, T. (2005). The cryptochromes. Genome Biol. **6:** 220.

Lin, W.H., Wang, Y., Mueller-Roeber, B., Brearley, C.A., Xu, Z.H., and Xue, H.W. (2005). At5PTase13 modulates cotyledon vein development through regulating auxin homeostasis. Plant Physiol. **139:** 1677–1691.

Lin, W.H., Ye, R., Ma, H., Xu, Z.H., and Xue, H.W. (2004). DNA chip-based expression profile analysis indicates involvement of the phosphatidylinositol signaling pathway in multiple plant responses to hormone and abiotic treatments. Cell Res. **14:** 34–45.

Liscum, E., and Briggs, W.R. (1995). Mutations in the NPH1 locus of Arabidopsis disrupt the perception of phototropic stimuli. Plant Cell **7:** 473–485.

Liscum, E., and Briggs, W.R. (1996). Mutations of *Arabidopsis* in potential transduction and response components of the phototropic signaling pathway. Plant Physiol. **112:** 291–296.

Liu, K., Li, L., and Luan, S. (2005). An essential function of phosphatidylinositol phosphates in activation of plant shaker-type K^+ channels. Plant J. **42:** 433–443.

Lou, Y., Gou, J.Y., and Xue, H.W. (2007). PIP5K9, an *Arabidopsis* phosphatidylinositol monophosphate kinase, interacts with a cytosolic invertase to negatively regulate sugar-mediated root growth. Plant Cell **19:** 163–181.

Love, J., Dodd, A.N., and Webb, A.A. (2004). Circadian and diurnal calcium oscillations encode photoperiodic information in *Arabidopsis.* Plant Cell **16:** 956–966.

Luan, S., Kudla, J., Rodriguez-Concepcion, M., Yalovsky, S., and Gruissem, W. (2002). Calmodulins and calcineurin B-like proteins: calcium sensors for specific signal response coupling in plants. Plant Cell **14**(Suppl): S389–S400.

Mao, J., Zhang, Y.C., Sang, Y., Li, Q.H., and Yang, H.Q. (2005). From The Cover: A role for *Arabidopsis* cryptochromes and COP1 in the regulation of stomatal opening. Proc. Natl. Acad. Sci. USA **102:** 12270–12275.

McNellis, T.W., Torii, K.U., and Deng, X.W. (1996). Expression of an N-terminal fragment of COP1 confers a dominant-negative effect on light-regulated seedling development in *Arabidopsis.* Plant Cell **8:** 1491–1503.

Meehan, L., Harkins, K., Chory, J., and Rodermel, S. (1996). Lhcb transcription is coordinated with cell size and chlorophyll accumulation (studies on fluorescence-activated, cell-sorter-purified single cells from wild-type and in mutans *Arabidopsis thaliana*). Plant Physiol. **112:** 953–963.

Møller, S.G., Kim, Y.S., Kunkel, T., and Chua, N.H. (2003). PP7 is a positive regulator of blue light signaling in *Arabidopsis.* Plant Cell **15:** 1111–1119.

Motchoulski, A., and Liscum, E. (1999). *Arabidopsis* NPH3: A NPH1 photoreceptor-interacting protein essential for phototropism. Science **286:** 961–964.

Murashige, T., and Skoog, F. (1962). A revised medium for rapid growth bioassays with tobacco tissue cultures. Physiol. Plant. **15:** 473–497.

Nam, K.H., and Li, J. (2002). BRI1/BAK1, a receptor kinase pair mediating brassinosteroid signaling. Cell **110:** 203–212.

Ohgishi, M., Saji, K., Okada, K., and Sakai, T. (2004). Functional analysis of each blue light receptor, cry1, cry2, phot1, and phot2, by using combinatorial multiple mutants in Arabidopsis. Proc. Natl. Acad. Sci. USA **101:** 2223–2228.

Parks, B.M., Cho, M.H., and Spalding, E.P. (1998). Two genetically separable phases of growth inhibition induced by blue light in *Arabidopsis* seedlings. Plant Physiol. **118:** 609–615.

Pedmale, U.V., and Liscum, E. (2007). Regulation of phototropic signaling in Arabidopsis via phosphorylation state changes in the phototropin 1-interacting protein NPH3. J. Biol. Chem. **282:** 19992–20001.

Poovaiah, B.W., Yang, T., and van Loon, J.J. (2002). Calcium/calmodulin-mediated gravitropic response in plants. J. Gravit. Physiol. **9:** 211–214.

Qin, Z.X., Chen, Q.J., Tong, Z., and Wang, X.C. (2005). The *Arabidopsis* inositol 1,3,4-trisphosphate 5/6 kinase, AtItpk-1, is involved in plant photomorphogenesis under red light conditions, possibly via interaction with COP9 signalosome. Plant Physiol. Biochem. **43:** 947–954.

Quan, R., Lin, H., Mendoza, I., Zhang, Y., Cao, W., Yang, Y., Shang, M., Chen, S., Pardo, J.M., and Guo, Y. (2007). SCABP8/CBL10, a putative calcium sensor, interacts with the protein kinase SOS2 to protect Arabidopsis shoots from salt stress. Plant Cell **19:** 1415–1431.

Rockwell, N.C., Su, Y.S., and Lagarias, J.C. (2006). Phytochrome structure and signaling mechanisms. Annu. Rev. Plant Biol. **57:** 837–858.

Rook, F., Gerrits, N., Kortstee, A., van Kampen, M., Borrias, M., Weisbeek, P., and Smeekens, S. (1998). Sucrose-specific signalling represses translation of the *Arabidopsis* ATB2 bZIP transcription factor gene. Plant J. **15:** 253–263.

Plieth, C. (2006). Aequorin as a reporter gene. Methods Mol. Biol. **323:** 307–327.

Reiter, W.D. (2002). Biosynthesis and properties of the plant cell wall. Curr. Opin. Plant Biol. **5:** 536–542.

Sakai, T., Wada, T., Ishiguro, S., and Okada, K. (2000). RPT2. A signal transducer of the phototropic response in *Arabidopsis.* Plant Cell **12:** 225–236.

Sanchez, J.P., and Chua, N.H. (2001). *Arabidopsis* PLC1 is required for secondary responses to abscisic acid signals. Plant Cell **13:** 1143–1154.

Sang, Y., Li, Q.H., Rubio, V., Zhang, Y.C., Mao, J., Deng, X.W., and Yang, H.Q. (2005). N-terminal domain-mediated homodimerization is required for photoreceptor activity of Arabidopsis CRYPTOCHROME 1. Plant Cell **17:** 1569–1584.

Sechi, A.S., and Wehland, J. (2000). The actin cytoskeleton and plasma membrane connection: PtdIns(4,5)P(2) influences cytoskeletal protein activity at the plasma membrane. J. Cell Sci. **21:** 3685–3695.

Schepens, I., Duek, P., and Fankhauser, C. (2004). Phytochrome-mediated light signalling in *Arabidopsis.* Curr. Opin. Plant Biol. **7:** 564–569.

Smyth, G.K. (2005). Limma: Linear models for microarray data. In Bioinformatics and Computational Biology Solutions Using R and Bioconductor, R. Gentlemen, V. Carey, S. Dudoit, R. Irizarry, and W. Huber, eds (New York: Springer), pp. 397–420.

Stepanova, A.N., and Alonso, J.M. (2005). Arabidopsis ethylene signaling pathway. Sci. STKE **2005:** cm4.

Stoelzle, S., Kagawa, T., Wada, M., Hedrich, R., and Dietrich, P. (2003). Blue light activates calcium-permeable channels in *Arabidopsis* mesophyll cells via the phototropin signaling pathway. Proc. Natl. Acad. Sci. USA **100:** 1456–1461.

Suh, S., Moran, N., and Lee, Y. (2000). Blue light activates potassium-efflux channels in flexor cells from *Samanea saman* motor organs via two mechanisms. Plant Physiol. **123:** 833–843.

Tan, X., Calderon-Villalobos, L.I., Sharon, M., Zheng, C., Robinson, C.V., Estelle, M., and Zheng, N. (2007). Mechanism of auxin perception by the TIR1 ubiquitin ligase. Nature **446:** 640–645.

Wang, H. (2005). Signaling mechanisms of higher plant photoreceptors: A structure-function perspective. Curr. Top. Dev. Biol. **68:** 227–261.

Wang, W.G., and Gu, J.B. (1986). Comparison of the methods for extracting ATP from plant leaves. Plant Physiol Commun. **5:** 54–55.

Weigel, D., and Glazebrook, J., eds (2002). Arabidopsis: A Laboratory Manual. (Cold Spring Harbor, NY: Cold Spring Harbor Laboratory Press).

Williams, M.E., Torabinejad, J., Cohick, E., Parker, K., Drake, E.J., Thompson, J.E., Hortter, M., and Dewald, D.B. (2005). Mutations in the *Arabidopsis* phosphoinositide phosphatase gene SAC9 lead to overaccumulation of PtdIns(4,5)P2 and constitutive expression of stress-response pathway. Plant Physiol. **138:** 686–700.

Wymer, C.L., Bibikova, T.N., and Gilroy, S. (1997). Cytoplasmic free calcium distributions during the development of root hairs of *Arabidopsis thaliana.* Plant J. **12:** 427–439.

Xu, X., Hotta, C.T., Dodd, A.N., Love, J., Sharrock, R., Lee, Y.W., Xie, Q., Johnson, C.H., and Webb, A.A. (2007). Distinct light and clock modulation of cytosolic free Ca^{2+} oscillations and rhythmic CHLOROPHYLL A/B BINDING PROTEIN2 promoter activity in *Arabidopsis.* Plant Cell **19:** 3474–3490.

Xue, H.W., Chen, X., and Li, G. (2007). Involvement of phospholipid signaling in plant growth and hormone effects. Curr. Opin. Plant Biol. **10:** 483–489.

Xue, H.W., Pical, C., Brearley, C., Elge, S., and Müller-Röber, B. (1999). A plant 126-kDa phosphatidylinositol 4-kinase with a novel repeat structure. Cloning and functional expression in baculovirus-infected insect cells. J. Biol. Chem. **274:** 5738–5745.

Yang, H.Q., Tang, R.H., and Cashmore, A.R. (2001). The signaling mechanism of *Arabidopsis* CRY1 involves direct interaction with COP1. Plant Cell **13:** 2573–2587.

Yang, T., and Poovaiah, B.W. (2003). Calcium/calmodulin-mediated signal network in plants. Trends Plant Sci. **8:** 505–512.

Yokoyama, R., Rose, J.K., and Nishitani, K. (2004). A surprising diversity and abundance of xyloglucan endotransglucosylase/hydrolases in rice. Classification and expression analysis. Plant Physiol. **134:** 1088–1099.

Zhong, R., Burk, D.H., Morrison III, W.H., and Ye, Z.H. (2004). FRAGILE FIBER3, an *Arabidopsis* gene encoding a type II inositol polyphosphate 5-phosphatase, is required for secondary wall synthesis and actin organization in fiber cells. Plant Cell **16:** 3242–3259.